


Altered pathways of keratinization, extracellular matrix generation, angiogenesis, and stromal stem cells proliferation in patients with systemic sclerosis

Journal of Scleroderma and
Related Disorders
2023, Vol. 8(2) 151–166
© The Author(s) 2022
Article reuse guidelines:
sagepub.com/journals-permissions
DOI: 10.1177/23971983221130145
journals.sagepub.com/home/jso


Amelia Spinella^{1*}, Domenico Lo Tartaro^{2*}, Lara Gibellini²,
Marco de Pinto¹ , Valentina Pinto³, Elisa Bonetti³, Francesca
Lolli³, Melba Lattanzi³ , Federica Lumetti¹, Gabriele Amati¹,
Giorgio De Santis^{2,3}, Andrea Cossarizza², Carlo Salvarani^{1,4,5}
and Dilia Giuggioli^{1,2} 

Abstract

Objective: Systemic sclerosis is characterized by endothelial dysfunction, autoimmunity abnormalities, and fibrosis of the skin and internal organs. The pathogenetic mechanisms underlying systemic sclerosis vasculopathy are still not clarified. A complex cellular and extracellular network of interactions has been studied, but it is currently unclear what drives the activation of fibroblasts/myofibroblasts and the extracellular matrix deposition.

Methods: Using RNA sequencing, the aim of the work was to identify potential functional pathways implied in systemic sclerosis pathogenesis and markers of endothelial dysfunction and fibrosis in systemic sclerosis patients. RNA-sequencing analysis was performed on RNA obtained from biopsies from three systemic sclerosis patients and three healthy controls enrolled in our University Hospital. RNA was used to generate sequencing libraries that were sequenced according to proper transcriptomic analyses. Subsequently, we performed gene set enrichment analysis of differentially expressed genes on the entire list of genes that compose the RNA-sequencing expression matrix.

Results: Gene set enrichment analysis revealed that healthy controls were characterized by gene signatures related to stromal stem cells proliferation, cytokine–cytokine receptor interaction, macrophage-enriched metabolic network, whereas systemic sclerosis tissues were enriched in signatures associated with keratinization, cornification, retinoblastoma 1 and tumor suppressor 53 signaling.

Conclusion: According to our data, RNA-sequencing and pathway analysis revealed that systemic sclerosis subjects display a discrete pattern of gene expression associated with keratinization, extracellular matrix generation, and negative regulation of angiogenesis and stromal stem cells proliferation. Further analysis on larger numbers of patients is needed; however, our findings provide an interesting framework for the development of biomarkers useful to explore potential future therapeutic approaches.

¹Scleroderma Unit and Rheumatology Unit, Medical School, University of Modena and Reggio Emilia, University Hospital of Modena Policlinico of Modena, Modena, Italy

²Department of Medical and Surgical Sciences of Children and Adults, University of Modena and Reggio Emilia, Modena, Italy

³Division of Plastic Surgery, University Hospital of Modena and Reggio Emilia Policlinico of Modena, Modena, Italy

⁴Department of Surgery, Medicine, Dentistry and Morphological Sciences with Transplant Surgery, Oncology and Regenerative Medicine Relevance, University of Modena and Reggio Emilia, Modena, Italy

⁵Rheumatology Unit, AUSL-IRCCS of Reggio Emilia, Reggio Emilia, Italy

*These authors have contributed equally to this work and share first authorship.

Corresponding author:

Dilia Giuggioli, Scleroderma Unit and Rheumatology Unit, Medical School, University of Modena and Reggio Emilia, University Hospital of Modena Policlinico of Modena, Modena, Italy.
Email: dilia.giuggioli@unimore.it

Keywords

Systemic sclerosis, RNA-sequencing analysis, gene expression, pathogenetic pathways

Date received: 24 July 2022; accepted: 15 September 2022

Introduction

Systemic sclerosis (SSc) is a rare and life-threatening connective tissue disease, characterized by endothelial dysfunction, autoimmunity abnormalities, and aberrant fibrosis of the skin and internal organs.^{1–3} Disease pathogenesis is characterized by early microvascular changes with endothelial cells (ECs) alteration, followed by dysfunctional mechanisms promoting their transition into myofibroblasts, the cells responsible for fibrosis and collagen deposition in the tissues.⁴ It has been observed that microvascular damage might be the first symptom of SSc; based on these factors, myofibroblast generation process may link two pivotal events in SSc: microvascular injury and fibrosis.⁵ Production of activating cytokines, disruption of vascular permeability with extravasation of growth factors, and induction of hypoxia possibly contribute to the pool of myofibroblasts through endothelial-to-mesenchymal transition. A complex autoimmune activation, involving innate and adaptive immunity with peculiar autoantibody production, also characterizes the disease.

To resume, a complex network of interactions between ECs, pericytes, myofibroblasts, and the extracellular matrix (ECM), together with growth factors and cytokines, participate in disease diffusion and evolution, but it is currently poorly clear what drives the activation of fibroblasts and the increased ECM deposition responsible for the fibrotic changes well known in SSc vasculopathy.^{6,7}

These modifications drive some of the most noticeable SSc clinical manifestations, such as Raynaud's phenomenon (RP), digital ulcers (DUs), and pulmonary arterial hypertension (PAH).^{6,7}

Altered gene expression seems to contribute to these aberrant mechanisms. Prior gene expression profiling studies and proteome-side analyses partially elucidated the molecular pathways affected in SSc patients.^{8,9} However, these studies do not account for cellular heterogeneity and differential cell composition of target tissues, and their results are limited.

Using RNA-sequencing (RNA-seq), our report aims to identify potential functional pathways possibly involved in SSc pathogenesis and markers that could potentially be used to better understand endothelial damage and fibrosis mechanisms in SSc patients.

Methods

Patients and healthy volunteers

Three SSc patients and three age- and sex-matched healthy controls (HCs) were enrolled in our University Hospital

between January 2019 and December 2020. Written informed consent was obtained from all of the participants. This study was approved by local ethical committees (protocol no. 275/2016) and performed in accordance with the latest version of the Helsinki declaration.

RNA extraction

Skin biopsies were performed under local anesthetic with a skin biopsy punch (size range, 2–5 mm), in the site-surgery (perioral skin) before autologous fat grafting (lipofilling) and one sample was taken at a time. The biopsy was transferred to a labeled cryovial that was then immediately immersed in liquid nitrogen. All samples were logged in accordance with standard operating procedures and stored in liquid nitrogen until use. Standard precautions to prevent contamination with RNases were employed. The sample was removed from the liquid nitrogen and transferred on dry ice. Samples were immediately placed into a tube containing stainless steel beads and cold lysis buffer (RLT) with beta-mercaptoethanol (RNeasy Plus Mini kit; Qiagen, Hilden, Germany). Samples were homogenized first in the TissueLyser LT (Qiagen) and then in the QIAshredder (Qiagen). Then, RNA was obtained using the RNeasy Plus Mini kit, following manufacturer's instructions. Eluted RNA was measured using the Nanodrop Microvolume Spectrophotometer and RNA quality was measured using a microfluidic gel electrophoresis chip (Bioanalyzer RNA 6000 Nano Chip, Agilent, UK). RNA integrity numbers were obtained with the software provided (2100 Expert Software) with the Agilent 2100 Bioanalyzer (Agilent, UK). For every sample, RNA integrity number (RIN) was >8 . A260/280 and A260/230 ratios were also obtained and were >1.9 for all samples.

Transcriptomic analyses

RNA from each sample was used to generate sequencing libraries that were sequenced using an Illumina HiSeq 2500, giving 30 million paired end reads per sample which were 100 bp in length. FASTQ files were checked for quality using FastQC version 0.11.9 and aligned using the splice aware aligner program STAR to generate alignment files (GENCODE Human Release 37, reference genome sequence GRCh38/hg38). The read counts for each sample file were obtained using the R package Rsubread v2.4.3. Differential gene expression analysis was carried out using edgeR package v3.32.1. Library size normalization by trimmed mean of M (TMM) values was performed using the "calcNormFactors" function embedded in edgeR. Differential gene expression was assessed using "exactTest" function of edgeR, using default parameters. Benjamini–Hochberg correction was applied to estimate the false discovery rate (FDR). Differentially expressed genes (DEGs) were selected using as threshold $FDR \leq 0.01$ and $\log_2FC > 1$. Gene ontology enrichment analysis was performed using clusterProfiler v4.2.2.

Table 1. Demographic and clinical data of SSc patients and HC.

Patients	SSc ³	HC ³
General features		
Mean age, $M \pm SD$ years (range)	51.3 \pm 8.1 (42–56)	50.6 \pm 6.6 (43–55)
Females	3 (100%)	3 (100%)
Mean disease duration, $M \pm SD$ years (range)	11.0 \pm 5.6 (6–17)	/
SSc subset		
Diffuse cutaneous	2 (66.7%)	/
Limited cutaneous	1 (33.3%)	/
Antibodies		
Scl-70	3 (100%)	/
Comorbidities		
None	/	3 (100%)
Digital ulcers	3 (100%)	/
Pulmonary hypertension	1 (33.3%)	/
Pulmonary fibrosis	2 (66.7%)	/
Treatments		
Prostanoids	3 (100%)	/
CCB	3 (100%)	/
ERA	2 (66.7%)	/
PDE5Inh	2 (66.7%)	/
DMARDs/bDMARDs	2 (66.7%)	/

SSc: systemic sclerosis; HC: healthy control; CCB: calcium channel blockers; ERA: endothelin receptor antagonist; PDE5Inh: phosphodiesterase type 5 inhibitors; DMARDs/bDMARDs: disease-modifying anti-rheumatic drugs traditional/biologics.

Gene set enrichment analysis

Gene set enrichment analysis (GSEA) was applied on the entire list of genes that compose the RNA-seq expression matrix. Genes were ranked based on their fold change calculated by pairwise comparison between HC and SSc groups, and analyzed by GSEA in pre-ranked mode. As enrichment statistic, we adopted a more conservative scoring approach by setting enrichment statistic = “classic,” which is the recommended approach for RNA-seq data. The number of permutations has been set to 1000, while Max size and Min size (to exclude larger or smaller sets) have been set to 500 and 15, respectively. To normalize the enrichment scores (ESs) across analyzed gene, we adopted “meandiv” mode. All gene sets of interest were retrieved from the curated signatures collection (c2.all.v7.1 and c5.all.v7.1) of the Molecular Signatures Database.

Digital cytometry

CIBERSORTx is a machine learning method and was used to impute cell fraction without physical cell isolation.¹⁰ Briefly, we built a custom matrix file with a human skin signature using a publicly available single-cell RNA-seq data set (GSE130973). Then, we used this matrix to infer cell fractions from our bulk RNA-seq samples. CIBERSORTx

was executed in “absolute mode” to calculate a score that reflects the absolute proportion of each cell type in our bulk RNA-seq mixture using 100 permutations (the quantile normalization was disabled as recommended for RNA-seq data).

Results

RNA-seq analysis was performed on RNA extracted from the biopsies obtained with a skin biopsy punch (size range, 2–5 mm) of three SSc female patients and three female HCs. Biopsies were performed in the site-surgery before autologous fat grafting (lipofilling) procedure for SSc subjects as SSc regenerative treatment for the face (mouth); while HC without comorbidities received various aesthetic face-lifting approaches with concomitant skin biopsies.

The demographic and clinical data of participants are listed in Table 1. The median ages were 51.3 \pm 8.1 *SD* years (range, 42–56) and 50.6 \pm 6.6 *SD* years (range, 43–55) for SSc cases and HC, respectively.

We performed DEGs analysis between SSc and HC, and we identified 305 DEGs that were up- or downregulated at least two-fold (Table 2). In particular, 175 genes were upregulated and 130 genes were downregulated (Table 2). A marked upregulation of genes involved in Wnt signaling, including Wnt family member (WNT) 4,

WNT9B, WNT3, WNT16, with 2.5-, 11.3-, 6.5-, 5.6-folds, respectively, was present in HC if compared with SSc (Table 2 and Figure 1). The upregulation of collagen type VI alpha 5 chain (COL6A5), Fos proto-oncogene, AP-1 transcription factor subunit (FOS), glycoprotein M6A (GPM6A), extracellular matrix protein 2 (ECM2), adhesion G protein-coupled receptor E3 (ADGRE3), vascular endothelial growth factor D (VEGFD), LIF interleukin 6 family cytokine (LIF), among others, was also observed (Table 2 and Figure 1). Conversely, a marked downregulation of late cornified envelope (LCE) 3D, LCE3E, LCE1E, with 22-, 26- and 22-folds, respectively, and of genes encoding for keratins, including keratin (KRT) 35, KRT38, KRT82, was present in HC versus SSc samples (Table 2 and Figure 1). Gene ontology enrichment analysis revealed that DEGs in SSc biopsies were enriched for gene sets involved in actin filament-based movement, actin-mediated cell contraction, actomyosin structure organization, cell response to toxic substance, among others (Figure 2).

To identify potential functional pathways that could be involved in SSc pathogenesis, we performed GSEA of DEGs. GSEA revealed that HCs were characterized, among others, by gene signatures related to stromal stem cells proliferation, cytokine–cytokine receptor interaction, macrophage-enriched metabolic network, whereas SSc samples were enriched in signatures related to keratinization, cornification, retinoblastoma (RB) 1 and tumor suppressor (TP) 53 signaling (Figure 3).

Cell subsets in which differential gene expression occurs were identified and quantified according to the CIBERSORTx algorithm (Figure 4). We found that DEGs were expressed in keratinocytes, epithelial stem cells (EpSC), fibroblasts, pericytes, and vascular endothelial cells (VECs), and that keratinocytes and fibroblasts in SSc, whereas EpSC and VECs were decreased (Figure 4).

Discussion

As introduced, altered gene expression seems to contribute to the aberrant mechanisms that propagate SSc vasculopathy.^{8,9} Recent advances in cell transcriptome technology, including RNA-seq analysis, seem to provide an unprecedented point of view into SSc pathogenesis and offer important implications for personalized disease management.¹¹

Here, we provided a comprehensive analysis of RNA-seq data derived from SSc and HCs skin tissues. According to our data, RNA-seq, differential gene expression and pathway analysis revealed that SSc subjects display a discrete pattern of gene expression associated with keratinization and ECM generation. In detail, according to GSEA, we demonstrated that HC were characterized by gene signatures related to stromal stem cells proliferation, cytokine–cytokine receptor interaction macrophage-enriched metabolic network, among others. On the other

hand, SSc tissues were added in signatures related to keratinization, cornification, RB 1 and TP 53 signaling, to the detriment of regulation of angiogenesis and stromal stem cells proliferation.

Various conditions characterized by aberrant fibrosis and vascular dysfunction, such as keloids, were also studied using RNA-seq.^{12,13} Results from these reports highlighted the roles of tumor growth factor beta (TGF- β) and Eph–ephrin signaling pathways in keloids processes; critical regulators probably involved, such as TWIST1, FOXO3, and SMAD3, were also identified. In addition, tumor-related pathways were activated and dysregulated in keloid fibroblasts and ECs, which could explain malignant features of keloids. These findings will help the clinicians to better recognize fibrotic skin pathogenesis and provide possible targets for fibrotic disease therapies.

Other connective tissue diseases, such as Sjögren's syndrome, were recently studied through transcriptomic, genomic, epigenetic, cytokine expression and flow cytometry data, to identify groups of patients with distinct patterns of immune dysregulation, in combination with clinical parameters. RNA-Seq was also used and the identified biomarkers were functional to evaluate response to treatments and to develop future target therapies.¹⁴

Identifying the specific immune mechanisms underlying SSc pathogenesis could similarly result in innovative therapies production that selectively target the aberrant immune response, with better efficacy and less toxicity. A comprehensive analysis of T-cell mediated immune responses in the affected skin of SSc patients was performed by means of single-cell RNA-seq with interesting results about distinct signaling activated pathways.¹⁵

Clinical implications are therefore mandatory. In 2019, some authors exploited single-cell RNA-seq by performing pathway analysis with GSEA and ingenuity pathway analysis (IPA) in SSc skin.¹² They finally demonstrated that the SSc EC expression profile is enriched in processes related to ECM generation and negative regulation of angiogenesis and epithelial-to-mesenchymal transition. Two of the top DEGs, HSPG2 and APLNR, were independently verified as potential markers of EC injury. These genes have been associated with vascular dysfunction and fibrosis in different settings, including SSc with its harmful complications, such as lung fibrosis and PAH.^{16–19}

As partially known, myofibroblasts are key effector cells in the remodeling process of interstitial lung disease (ILD) associated with SSc. Transcriptomic analysis using single-cell RNA-seq was performed by some authors²⁰ to define the transcriptomes of myofibroblasts and other mesenchymal cells in SSc to clarify how alterations in fibroblast phenotypes lead to SSc-ILD fibrosis. Results from this study established a great previously unrecognized fibroblast heterogeneity in SSc-ILD and described multimodal transcriptome-phenotypes associated with

Table 2. Differentially expressed genes between HC and SSC.

Entrezid	Symbol	Gene name	logFC	P value
101926892	LOC101926892	Uncharacterized LOC101926892	8.85	9.64E-11
155	ADRB3	Adrenoceptor beta 3	7.63	1.50E-05
402381	SOHLH1	Spermatogenesis and oogenesis-specific basic helix-loop-helix 1	7.57	5.30E-08
84658	ADGRE3	Adhesion G protein-coupled receptor E3	5.56	3.24E-07
23547	LILRA4	Leukocyte immunoglobulin-like receptor A4	5.48	7.33E-09
400120	SERTM1	Serine-rich and transmembrane domain containing 1	5.31	2.53E-07
3045	HBD	Hemoglobin subunit delta	4.97	4.43E-09
101929777	LOC101929777	Uncharacterized LOC101929777	4.77	1.51E-07
1360	CPBI	Carboxypeptidase B1	4.69	8.72E-05
3043	HBB	Hemoglobin subunit beta	4.68	1.25E-08
101927350	LINC01254	Long intergenic non-protein-coding RNA 1254	4.65	3.05E-12
404266	HOXB-AS3	HOXB cluster antisense RNA 3	4.54	8.47E-05
1178	CLC	Charcot-Leyden crystal galectin	4.54	1.71E-05
8785	MATN4	Matrilin 4	4.50	1.51E-07
3040	HBA2	Hemoglobin subunit alpha 2	4.31	2.15E-08
340273	ABCB5	ATP-binding cassette subfamily B member 5	4.30	6.29E-09
3952	LEP	Leptin	4.25	2.93E-05
3039	HBA1	Hemoglobin subunit alpha 1	4.21	2.76E-09
25975	EGFL6	EGF-like domain multiple 6	4.14	8.03E-06
80763	SPX	Spexin hormone	4.07	0.00011464
389903	CSAG3	CSAG family member 3	4.06	1.58E-05
345275	HSD17B13	Hydroxysteroid 17-beta dehydrogenase 13	3.81	8.78E-12
931	MS4A1	Membrane spanning 4-domains A1	3.77	2.22E-07
60675	PROK2	Prokineticin 2	3.67	1.43E-05
933	CD22	CD22 molecule	3.57	3.20E-05
201516	ZSCAN4	Zinc finger and SCAN domain containing 4	3.50	7.55E-06
7484	WNT9B	Wnt family member 9B	3.47	3.95E-12
60385	TSKS	Testis-specific serine kinase substrate	3.47	0.000538562
114043	TSPEAR-AS2	TSPEAR antisense RNA 2	3.44	6.00E-05
54084	TSPEAR	Thrombospondin-type laminin G domain and EAR repeats	3.36	2.34E-06
1046	CDX4	Caudal type homeobox 4	3.36	0.000517385
8972	MGAM	Maltase-glucoamylase	3.35	3.80E-07
10249	GLYAT	Glycine-N-acyltransferase	3.34	5.20E-05
8875	VNN2	Vanin 2	3.33	4.32E-06
64407	RGS18	Regulator of G protein signaling 18	3.31	1.57E-05
6530	SLC6A2	Solute carrier family 6 member 2	3.25	3.71E-14
256076	COL6A5	Collagen type VI alpha 5 chain	3.10	1.16E-05
79865	TREML2	Triggering receptor expressed on myeloid cells like 2	3.09	7.98E-05
100294720	NHEG1	Neuroblastoma highly expressed 1	3.05	1.59E-05
1002	CDH4	Cadherin 4	3.03	2.50E-05
64167	ERAP2	Endoplasmic reticulum aminopeptidase 2	2.98	7.49E-12
1441	CSF3R	Colony stimulating factor 3 receptor	2.91	1.64E-06
26166	RGS22	Regulator of G protein signaling 22	2.90	5.99E-05
30009	TBX21	T-box 21	2.84	6.12E-05
94031	HTRA3	HtrA serine peptidase 3	2.83	0.000107899
10578	GNLY	Granulysin	2.81	0.000267073
114780	PKD1L2	Polycystin 1 like 2 (gene/pseudogene)	2.78	0.000744359
23743	BHMT2	Betaine-homocysteine S-methyltransferase 2	2.77	0.000709063
7473	WNT3	Wnt family member 3	2.77	1.39E-11
9597	SMAD5-AS1	SMAD5 antisense RNA 1	2.72	3.10E-10
26577	PCOLCE2	Procollagen C-endopeptidase enhancer 2	2.71	0.000187824
3202	HOXA5	Homeobox A5	2.69	0.000581136
2353	FOS	Fos proto-oncogene, AP-1 transcription factor subunit	2.66	0.00025139

(Continued)

Table 2. (Continued)

Entrezid	Symbol	Gene name	logFC	P value
2219	FCN1	Ficolin 1	2.64	8.76E-05
5593	PRKG2	Protein kinase cGMP-dependent 2	2.63	2.73E-07
969	CD69	CD69 molecule	2.62	1.23E-06
2999	GZMH	Granzyme H	2.62	0.000205026
10631	POSTN	Periostin	2.61	0.000446456
2668	GDNF	Glial cell-derived neurotrophic factor	2.61	3.05E-05
146556	C16orf89	Chromosome 16 open reading frame 89	2.60	0.00037576
221476	PI16	Peptidase inhibitor 16	2.60	0.000200419
6402	SELL	Selectin L	2.60	2.58E-07
1805	DPT	Dermatopontin	2.60	9.67E-05
4969	OGN	Osteoglycin	2.59	1.43E-05
93035	PKHD1L1	PKHD1 like 1	2.58	1.93E-05
3953	LEPR	Leptin receptor	2.55	3.48E-09
11027	LILRA2	Leukocyte immunoglobulin like receptor A2	2.54	5.36E-05
3976	LIF	LIF interleukin 6 family cytokine	2.54	1.38E-07
29909	GPR171	G protein-coupled receptor 171	2.51	3.73E-05
100130231	LINC00861	Long intergenic non-protein coding RNA 861	2.51	0.000196239
51554	ACKR4	Atypical chemokine receptor 4	2.50	5.31E-05
9796	PHYHIP	Phytanoyl-CoA 2-hydroxylase interacting protein	2.50	1.75E-06
51384	WNT16	Wnt family member 16	2.49	4.62E-06
91851	CHRDL1	Chordin like 1	2.47	0.000492589
206338	LVRN	Laeverin	2.46	0.00082358
1066	CES1	Carboxylesterase 1	2.39	0.000609521
2823	GPM6A	Glycoprotein M6A	2.35	0.000234398
3575	IL7R	Interleukin 7 receptor	2.35	0.000342746
54857	GDPD2	Glycerophosphodiester phosphodiesterase domain containing 2	2.35	8.63E-06
53829	P2RY13	Purinergic receptor P2Y13	2.30	4.83E-05
3119	HLA-DQB1	Major histocompatibility complex, class II, DQ beta 1	2.30	1.30E-07
4069	LYZ	Lysozyme	2.28	1.50E-07
161753	ODF3L1	Outer dense fiber of sperm tails 3 like 1	2.28	0.000810101
5540	NPY4R	Neuropeptide Y receptor Y4	2.26	4.25E-05
440738	MAP1LC3C	Microtubule-associated protein 1 light chain 3 gamma	2.25	0.000553398
10800	CYSLTR1	Cysteinyl leukotriene receptor 1	2.20	4.50E-06
286530	P2RY8	P2Y receptor family member 8	2.19	0.000221151
1842	ECM2	Extracellular matrix protein 2	2.19	0.000420098
5551	PRF1	Perforin 1	2.18	0.000531069
151887	CCDC80	Coiled-coil domain containing 80	2.15	0.000242366
399823	FOXI2	Forkhead box I2	2.13	0.000413967
54518	APBB1IP	Amyloid beta precursor protein binding family B member 1 interacting protein	2.11	0.00044138
118738	ZNF488	Zinc finger protein 488	2.11	0.000419495
3561	IL2RG	Interleukin 2 receptor subunit gamma	2.10	3.58E-05
10686	CLDN16	Claudin 16	2.09	4.44E-05
3683	ITGAL	Integrin subunit alpha L	2.08	0.000509098
3687	ITGAX	Integrin subunit alpha X	2.07	0.000174999
94234	FOXQ1	Forkhead box Q1	2.06	5.87E-10
117289	TAGAP	T-cell activation Rho GTPase activating protein	2.04	6.58E-05
8434	RECK	Reversion inducing cysteine rich protein with kazal motifs	2.04	2.48E-05
6352	CCL5	C-C motif chemokine ligand 5	2.00	0.000219667
90865	IL33	Interleukin 33	2.00	3.95E-08
5794	PTPRH	Protein tyrosine phosphatase receptor type H	1.97	0.000693056
2326	FMO1	Flavin containing monooxygenase 1	1.97	2.38E-08
6366	CCL21	C-C motif chemokine ligand 21	1.96	1.24E-06

(Continued)

Table 2. (Continued)

Entrezid	Symbol	Gene name	logFC	P value
2124	EVI2B	Ecotropic viral integration site 2B	1.95	6.78E-05
64333	ARHGAP9	Rho GTPase activating protein 9	1.94	8.27E-05
100379345	MIR181A2HG	MIR181A2 host gene	1.92	0.000817622
440584	SLC2A1-AS1	SLC2A1 antisense RNA 1	1.91	0.000137611
1043	CD52	CD52 molecule	1.90	0.000310066
57007	ACKR3	Atypical chemokine receptor 3	1.90	1.74E-05
7940	LST1	Leukocyte-specific transcript 1	1.89	5.80E-05
2192	FBLN1	Fibulin 1	1.89	0.00038501
55713	ZNF334	Zinc finger protein 334	1.88	2.44E-05
11118	BTN3A2	Butyrophilin subfamily 3 member A2	1.88	2.48E-08
403323	LOC403323	Uncharacterized LOC403323	1.87	0.000255561
10090	UST	Uronyl 2-sulfotransferase	1.87	3.44E-09
643650	LINC00842	Long intergenic non-protein coding RNA 842	1.86	0.000183802
728643	HNRNPA1P33	Heterogeneous nuclear ribonucleoprotein A1 pseudogene 33	1.86	1.36E-07
23531	MMD	Monocyte to macrophage differentiation associated	1.82	0.000727749
129049	SGSM1	Small G protein signaling modulator 1	1.81	2.12E-05
5788	PTPRC	Protein tyrosine phosphatase receptor type C	1.80	0.000102226
55026	TMEM255A	Transmembrane protein 255A	1.79	0.000135186
123591	TMEM266	Transmembrane protein 266	1.77	0.000298357
120425	JAML	Junction adhesion molecule like	1.76	4.07E-05
79626	TNFAIP8L2	TNF-alpha-induced protein 8 like 2	1.76	0.000298517
10320	IKZFI	IKAROS family zinc finger 1	1.72	0.000830127
9098	USP6	Ubiquitin-specific peptidase 6	1.71	0.00013812
6252	RTNI	Reticulon 1	1.70	0.000642901
11119	BTN3A1	Butyrophilin subfamily 3 member A1	1.68	5.19E-06
1524	CX3CR1	C-X3C motif chemokine receptor 1	1.67	0.000852827
26157	GIMAP2	GTPase, IMAP family member 2	1.66	0.000169944
79891	ZNF671	Zinc finger protein 671	1.66	0.000260642
3117	HLA-DQA1	Major histocompatibility complex, class II, DQ alpha 1	1.63	4.20E-05
388011	LINC01550	Long intergenic non-protein coding RNA 1550	1.61	0.000368953
8935	SKAP2	Src kinase-associated phosphoprotein 2	1.60	1.85E-05
10384	BTN3A3	Butyrophilin subfamily 3 member A3	1.59	5.40E-05
27306	HPGDS	Hematopoietic prostaglandin D synthase	1.59	0.000213676
55244	SLC47A1	Solute carrier family 47 member 1	1.58	0.000876973
101927164	LOC101927164	Uncharacterized LOC101927164	1.58	6.33E-05
7058	THBS2	Thrombospondin 2	1.53	1.82E-05
57758	SCUBE2	Signal peptide, CUB domain, and EGF-like domain containing 2	1.53	3.22E-05
963	CD53	CD53 molecule	1.50	0.000642744
54504	CPVL	Carboxypeptidase vitellogenic like	1.49	3.32E-05
2530	FUT8	Fucosyltransferase 8	1.48	1.93E-05
2625	GATA3	GATA-binding protein 3	1.47	5.22E-05
6453	ITSN1	Intersectin 1	1.45	0.000168102
5997	RGS2	Regulator of G protein signaling 2	1.44	3.56E-05
79901	CYBRD1	Cytochrome b reductase 1	1.43	0.000662612
53833	IL20RB	Interleukin 20 receptor subunit beta	1.42	0.000208175
1520	CTSS	Cathepsin S	1.40	0.000105691
10866	HCP5	HLA complex P5	1.38	1.56E-05
5328	PLAU	Plasminogen activator, urokinase	1.38	0.000448423
28971	AAMDC	Adipogenesis-associated Mth938 domain containing	1.36	2.19E-05
6571	SLC18A2	Solute carrier family 18 member A2	1.34	4.92E-05
51302	CYP39A1	Cytochrome P450 family 39 subfamily A member 1	1.30	0.000753341

(Continued)

Table 2. (Continued)

Entrezid	Symbol	Gene name	logFC	P value
51097	SCCPDH	Saccharopine dehydrogenase (putative)	1.30	0.000160085
54361	WNT4	Wnt family member 4	1.30	0.000167086
7805	LAPTM5	Lysosomal protein transmembrane 5	1.28	0.000372444
4688	NCF2	Neutrophil cytosolic factor 2	1.25	5.32E-05
90634	N4BP2LI	NEDD4-binding protein 2 like 1	1.24	0.000709105
3176	HNMT	Histamine N-methyltransferase	1.22	0.000848657
79734	KCTD17	Potassium channel tetramerization domain containing 17	1.22	0.000714539
493812	HCG11	HLA complex group 11	1.22	0.000212103
131616	TMEM42	Transmembrane protein 42	1.22	0.000859229
7128	TNFAIP3	TNF-alpha-induced protein 3	1.19	0.000609645
9536	PTGES	Prostaglandin E synthase	1.19	0.000670154
79690	GAL3ST4	Galactose-3-O-sulfotransferase 4	1.19	0.000663895
9891	NUAK1	NUAK family kinase 1	1.18	0.000205103
6304	SATB1	SATB homeobox 1	1.17	4.63E-05
4088	SMAD3	SMAD family member 3	1.14	5.50E-05
4792	NFKBIA	NFKB inhibitor alpha	1.08	0.000807994
2619	GAS1	Growth arrest-specific 1	1.08	0.000508176
9805	SCRNI	Secernin 1	1.04	0.000197048
153020	RASGEF1B	RasGEF domain family member 1B	1.01	0.000580739
57475	PLEKHH1	Pleckstrin homology, MyTH4 and FERM domain containing H1	-1.08	0.000666038
23223	RRP12	Ribosomal RNA processing 12 homolog	-1.14	0.000181227
50487	PLA2G3	Phospholipase A2 group III	-1.19	0.000544955
5507	PPP1R3C	Protein phosphatase 1 regulatory subunit 3C	-1.20	0.000443646
54751	FBLIM1	Filamin-binding LIM protein 1	-1.27	0.000580775
5187	PER1	Period circadian regulator 1	-1.29	6.01E-05
11254	SLC6A14	Solute carrier family 6 member 14	-1.36	0.000117055
3371	TNC	Tenascin C	-1.42	0.000164153
8497	PPFIA4	PTPRF-interacting protein alpha 4	-1.42	0.000453085
151354	LRATD1	LRAT domain containing 1	-1.43	1.01E-05
3768	KCNJ12	Potassium voltage-gated channel subfamily J member 12	-1.43	0.000693952
84254	CAMKK1	Calcium/calmodulin dependent protein kinase 1	-1.44	4.13E-05
10804	GJB6	Gap junction protein beta 6	-1.50	1.83E-06
5208	PFKFB2	6-phosphofructo-2-kinase/fructose-2,6-biphosphatase 2	-1.53	0.000797632
79017	GGCT	Gamma-glutamylcyclotransferase	-1.58	0.000306746
8863	PER3	Period circadian regulator 3	-1.61	6.62E-07
158158	RASEF	RAS and EF-hand domain containing	-1.61	0.000109187
9687	GREB1	Growth regulating estrogen receptor binding 1	-1.62	0.000385599
8153	RND2	Rho family GTPase 2	-1.63	0.000167306
402778	IFITM10	Interferon-induced transmembrane protein 10	-1.73	0.000119745
7804	LRP8	LDL receptor-related protein 8	-1.77	0.000438195
374383	NCR3LG1	Natural killer cell cytotoxicity receptor 3 ligand 1	-1.85	0.000645021
22979	EFR3B	EFR3 homolog B	-1.86	0.000757246
118430	MUCL1	Mucin like 1	-1.87	0.000104517
11226	GALNT6	Polypeptide N-acetylgalactosaminyltransferase 6	-1.96	4.03E-08
192683	SCAMP5	Secretory carrier membrane protein 5	-1.97	0.000664492
7227	TRPS1	Transcriptional repressor GATA binding 1	-1.99	5.48E-07
29842	TFCP2L1	Transcription factor CP2 like 1	-2.03	0.000123612
1285	COL4A3	Collagen type IV alpha 3 chain	-2.06	0.000635889
6706	SPRR2G	Small proline rich protein 2G	-2.06	2.71E-08
84940	CORO6	Coronin 6	-2.10	3.02E-05
765	CA6	Carbonic anhydrase 6	-2.12	0.000432192
83694	RPS6KLI	Ribosomal protein S6 kinase like 1	-2.13	0.000374012

(Continued)

Table 2. (Continued)

Entrezid	Symbol	Gene name	logFC	P value
84676	TRIM63	Tripartite motif containing 63	-2.13	0.000360823
2171	FABP5	Fatty acid-binding protein 5	-2.15	3.69E-08
3485	IGFBP2	Insulin-like growth factor binding protein 2	-2.16	0.000844872
65009	NDRG4	NDRG family member 4	-2.17	1.40E-05
79801	SHCBP1	SHC-binding and spindle-associated 1	-2.22	1.06E-06
148523	CIART	Circadian-associated repressor of transcription	-2.23	2.24E-06
23657	SLC7A11	Solute carrier family 7 member 11	-2.30	0.00084804
23553	HYAL4	Hyaluronidase 4	-2.35	0.0003367
153478	PLEKHG4B	Pleckstrin homology and RhoGEF domain containing G4B	-2.45	8.71E-05
285489	DOK7	Docking protein 7	-2.48	0.000470274
1734	DIO2	Iodothyronine deiodinase 2	-2.49	1.55E-09
128488	WFDC12	WAP four-disulfide core domain 12	-2.51	6.12E-06
383	ARG1	Arginase 1	-2.52	0.000109898
5820	PVT1	Pvt1 oncogene	-2.53	1.18E-07
1745	DLX1	Distal-less homeobox 1	-2.53	2.58E-05
4824	NKX3-1	NK3 homeobox 1	-2.53	3.60E-06
5789	PTPRD	Protein tyrosine phosphatase receptor type D	-2.54	0.000681882
202299	LINC01554	Long intergenic non-protein coding RNA 1554	-2.56	6.65E-08
1769	DNAH8	Dynein axonemal heavy chain 8	-2.57	0.000468749
1594	CYP27B1	Cytochrome P450 family 27 subfamily B member 1	-2.57	0.000213961
144406	WDR66	WD repeat domain 66	-2.57	2.70E-05
56475	RPRM	Reprimo, TP53 dependent G2 arrest mediator homolog	-2.58	0.000851815
1768	DNAH6	Dynein axonemal heavy chain 6	-2.62	0.000295338
10218	ANGPTL7	Angiopoietin like 7	-2.71	0.000517742
338667	VSIG10L2	V-set and immunoglobulin domain containing 10 like 2	-2.73	0.000311392
9615	GDA	Guanine deaminase	-2.77	3.70E-05
4440	MSI1	Musashi RNA binding protein 1	-2.77	0.000188836
140807	KRT72	Keratin 72	-2.79	0.000245768
3755	KCNGB1	Potassium voltage-gated channel modifier subfamily G member 1	-2.82	0.000372192
27132	CPNE7	Copine 7	-2.86	1.29E-05
387700	SLC16A12	Solute carrier family 16 member 12	-2.87	0.000433402
387695	C10orf99	Chromosome 10 open reading frame 99	-2.88	0.000337971
6861	SYT5	Synaptotagmin 5	-2.89	0.000463435
148281	SYT6	Synaptotagmin 6	-2.92	0.000302434
319101	KRT73	Keratin 73	-3.00	2.30E-05
105377774	LOC105377774	Uncharacterized LOC105377774	-3.04	0.000113072
387911	CIQTNF9B	CIq and TNF-related 9B	-3.04	0.000748625
9720	CCDC144A	Coiled-coil domain containing 144A	-3.06	0.000102105
4753	NELL2	Neural EGFL-like 2	-3.07	1.69E-05
1301	COL11A1	Collagen type XI alpha 1 chain	-3.09	4.71E-08
105373551	LOC105373551	Uncharacterized LOC105373551	-3.12	1.12E-06
339768	ESPNL	Espin like	-3.14	0.000376495
339535	LINC01139	Long intergenic non-protein coding RNA 1139	-3.22	2.36E-07
121506	ERP27	Endoplasmic reticulum protein 27	-3.23	6.16E-08
2569	GABRR1	Gamma-aminobutyric acid type A receptor rho1 subunit	-3.29	0.0003984
100506217	NA	NA	-3.30	0.000674811
57016	AKR1B10	Aldo-keto reductase family 1 member B10	-3.30	8.00E-07
7545	ZIC1	Zic family member 1	-3.31	0.000392413
255324	EPGN	Epithelial mitogen	-3.32	0.000478875
163351	GBP6	Guanylate-binding protein family member 6	-3.36	4.40E-08
55584	CHRNA9	Cholinergic receptor nicotinic alpha 9 subunit	-3.37	0.000303345

(Continued)

Table 2. (Continued)

Entrezid	Symbol	Gene name	logFC	P value
64208	POPDC3	Popeye domain containing 3	-3.44	0.00021796
176	ACAN	Aggrecan	-3.47	0.000526066
401074	LINC00960	Long intergenic non-protein coding RNA 960	-3.47	5.96E-05
80309	SPHKAP	SPHK1 interactor, AKAP domain containing	-3.48	1.57E-06
84107	ZIC4	Zic family member 4	-3.51	0.000138626
729522	AACSP1	Acetoacetyl-CoA synthetase pseudogene 1	-3.57	5.13E-06
92736	OTOP2	Otopetrin 2	-3.66	5.50E-07
1143	CHRNB4	Cholinergic receptor nicotinic beta 4 subunit	-3.72	0.000636152
160762	CCDC63	Coiled-coil domain containing 63	-3.79	0.000458776
353134	LCE1D	Late cornified envelope 1D	-3.80	3.35E-08
121391	KRT74	Keratin 74	-3.92	0.000638024
162632	USP32P1	Ubiquitin-specific peptidase 32 pseudogene 1	-4.01	3.80E-09
4703	NEB	Nebulin	-4.03	0.000467365
54207	KCNK10	Potassium two pore domain channel subfamily K member 10	-4.07	0.000717882
353135	LCE1E	Late cornified envelope 1E	-4.20	5.96E-09
84648	LCE3D	Late cornified envelope 3D	-4.25	2.21E-26
191585	PLAC4	Placenta enriched 4	-4.37	1.86E-05
57795	BRINP2	BMP/retinoic acid inducible neural-specific 2	-4.40	0.000184955
146802	SLC47A2	Solute carrier family 47 member 2	-4.57	1.75E-10
102724541	NA	NA	-4.61	1.55E-08
4747	NEFL	Neurofilament light	-4.64	0.000177839
84221	SPATC1L	Spermatogenesis and centriole-associated 1 like	-4.73	4.27E-08
353145	LCE3E	Late cornified envelope 3E	-4.78	4.73E-22
84560	MT4	Metallothionein 4	-4.80	0.000461366
440482	ANKRD20A5P	Ankyrin repeat domain 20 family member A5, pseudogene	-4.94	0.00019383
347741	OTOP3	Otopetrin 3	-4.96	2.07E-14
57586	SYT13	Synaptotagmin 13	-5.15	3.77E-05
93273	LEMD1	LEM domain containing 1	-5.30	0.000528385
389668	XKR9	XK-related 9	-5.31	4.64E-10
3359	HTR3A	5-hydroxytryptamine receptor 3A	-5.44	1.19E-06
1311	COMP	Cartilage oligomeric matrix protein	-5.54	3.22E-15
7273	TTN	Titin	-5.79	2.27E-05
58503	OPRPN	Opiorphin prepropeptide	-5.81	0.000471129
4151	MB	Myoglobin	-6.16	0.000584199
487	ATP2A1	ATPase sarcoplasmic/endoplasmic reticulum Ca ²⁺ transporting 1	-6.27	0.000323427
643224	TUBBP5	Tubulin beta pseudogene 5	-6.35	3.12E-13
779	CACNA1S	Calcium voltage-gated channel subunit alpha 1S	-6.65	0.000296762
4604	MYBPC1	Myosin-binding protein C, slow type	-6.78	0.000336416
116	ADCYAP1	Adenylate cyclase activating polypeptide 1	-6.78	0.000849582
200407	CREG2	Cellular repressor of E1A-stimulated genes 2	-7.12	0.000146125
146481	FRG2DP	FSHD region gene 2 family member D, pseudogene	-7.16	5.70E-09
8557	TCAP	Titin-cap	-8.00	0.000875387
284233	CYP4F35P	Cytochrome P450 family 4 subfamily F member 35, pseudogene	-8.47	2.28E-06
442721	LMOD2	Leiomodin 2	-9.63	0.000789905
58	ACTA1	Actin alpha 1, skeletal muscle	-10.85	0.000190824
4620	MYH2	Myosin heavy chain 2	-11.41	0.000552856

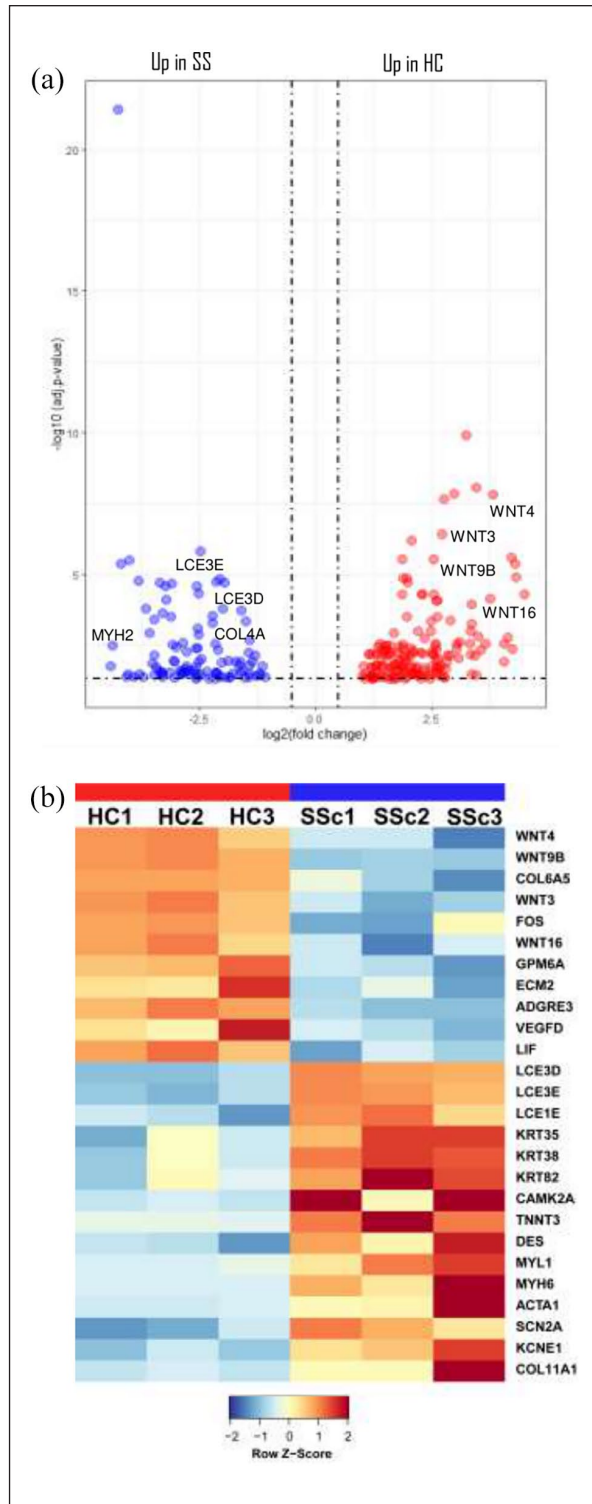


Figure 1. mRNA expression profiling of skin biopsies from HC and SSc patients: (a) volcano plot showing differentially expressed genes in healthy controls (HCs) and systemic sclerosis (SSc) patients and (b) gene expression heatmap of differentially expressed mRNAs in HC versus SSc tissues. Columns show each patient/individuals (red indicates healthy control (HC); blue indicates systemic sclerosis (SSc) patients). Rows show individual genes. The color of het varies from blue (i.e. downregulated expression) to red (i.e. upregulated expression).

these cells. These data considerably highlighted that myofibroblast differentiation and proliferation are crucial pathological mechanisms driving fibrosis in SSc-ILD with interesting new comprehensions into their functional role.²⁰ Similar findings were also observed in idiopathic pulmonary fibrosis (IPF).²¹

EC dysfunction efforts the initiation and contributes to the propagation of PAH too. Integrated analyses, including RNA-seq, aimed to provide a comprehensive atlas of EC in the health lung and PAH condition. These analyses revealed in detail that PAH-induced EC transcriptomic changes could provide novel targets for therapeutic development.^{22,23}

SSc is a rare detrimental disease which offers a challenging study model to speculate into pathologic angiogenesis and fibrogenesis processes.²⁴ SSc-related complications, such as skin ulcers, ILD, and PAH, still represent frequent causes of morbidity and mortality.^{3,25} In our experience, we analyzed scleroderma spectrum with special focus on the above conditions and their proper approaches and innovative treatment proposals.²⁶⁻³⁰ A critical and detailed analysis of such complications is necessary to pursue a personalized therapeutic strategy. Rapid progress in sequencing technologies in recent years provided valuable insights into complex biological systems with interesting potential medical applications and treatment implications.³¹

Our SSc subjects underwent autologous fat grafting procedure as SSc regenerative medicine approach to treat their cutaneous scleroderma-related manifestations. According to our preliminary findings, RNA-seq and pathway analysis particularly revealed that SSc subjects displayed a pattern of gene expression associated with keratinization and ECM generation. GSEA also established that SSc tissues were enriched in signatures related to keratinization and cornification, at the expense of regulation of angiogenesis and stromal stem cells proliferation.

These findings are in line with the proposed pathogenetic mechanisms underlying SSc, especially highlighting the importance of extracellular microenvironment imbalance and cells interaction, which leads to impaired angiogenesis, endothelial and epithelial to mesenchymal transition, fibroblast activation and ECM deposition, finally resulting in fibrosis.

The present study has several limitations. The first limitation is the low number of patients with heterogeneous disease duration used for the analysis, who were chosen on the basis of similar clinical features. Second, functional analysis is needed to clarify the roles of the identified possible pathogenetic mechanisms in SSc. However, our results provide an interesting framework for the identification of valuable biomarkers representing vascular damage and fibrotic alterations in SSc to explore future perspectives and therapeutic targets.



Figure 2. Dot plot of enriched pathways in HC versus SSc tissues.

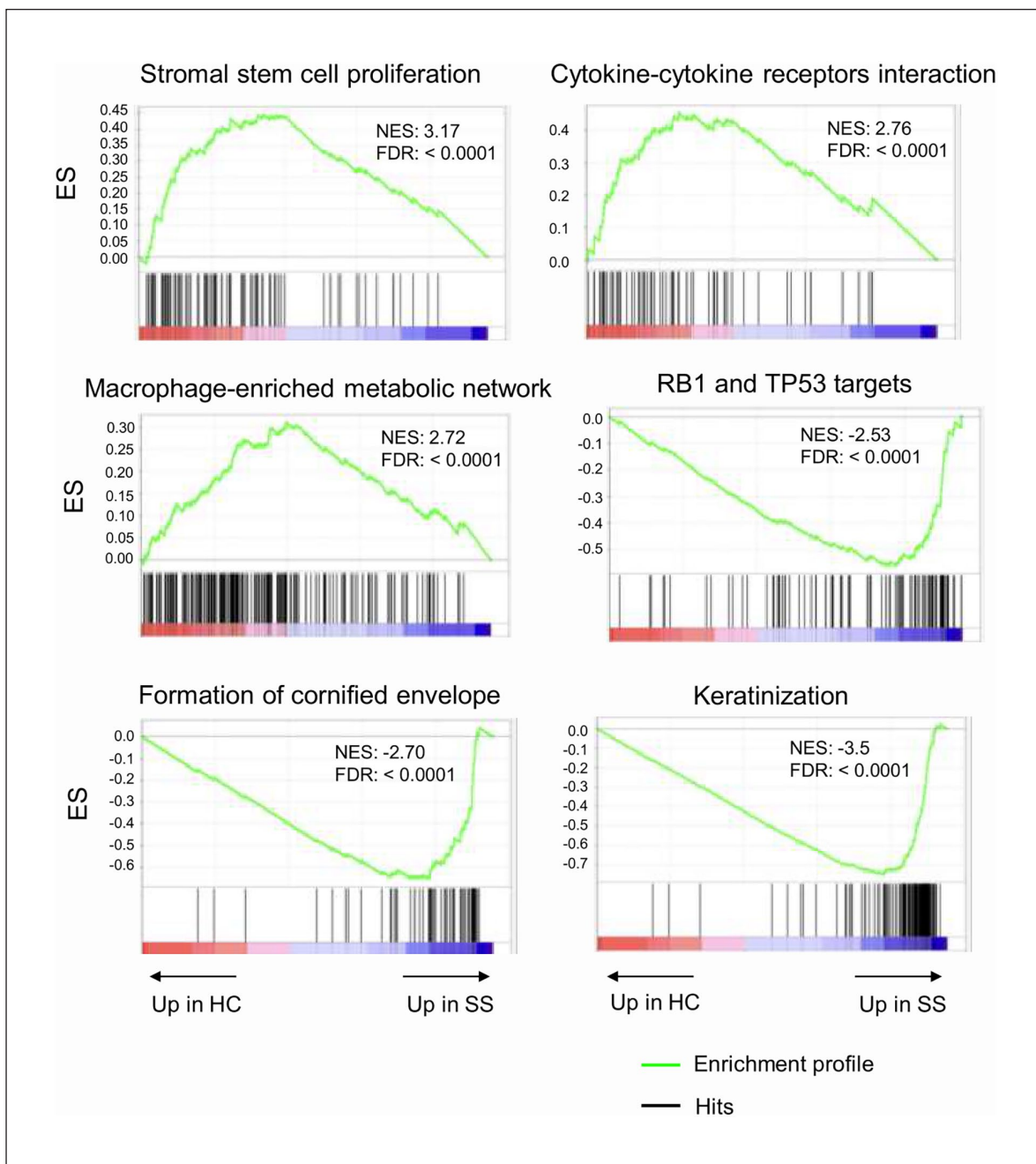


Figure 3. Gene set enrichment analysis (GSEA) in HC versus SSc tissues.

Enrichment of gene signature was analyzed in transcriptomic data from HC and SSc samples. ES: enrichment score; NES: normalized enrichment score; FDR: false discovery rate.

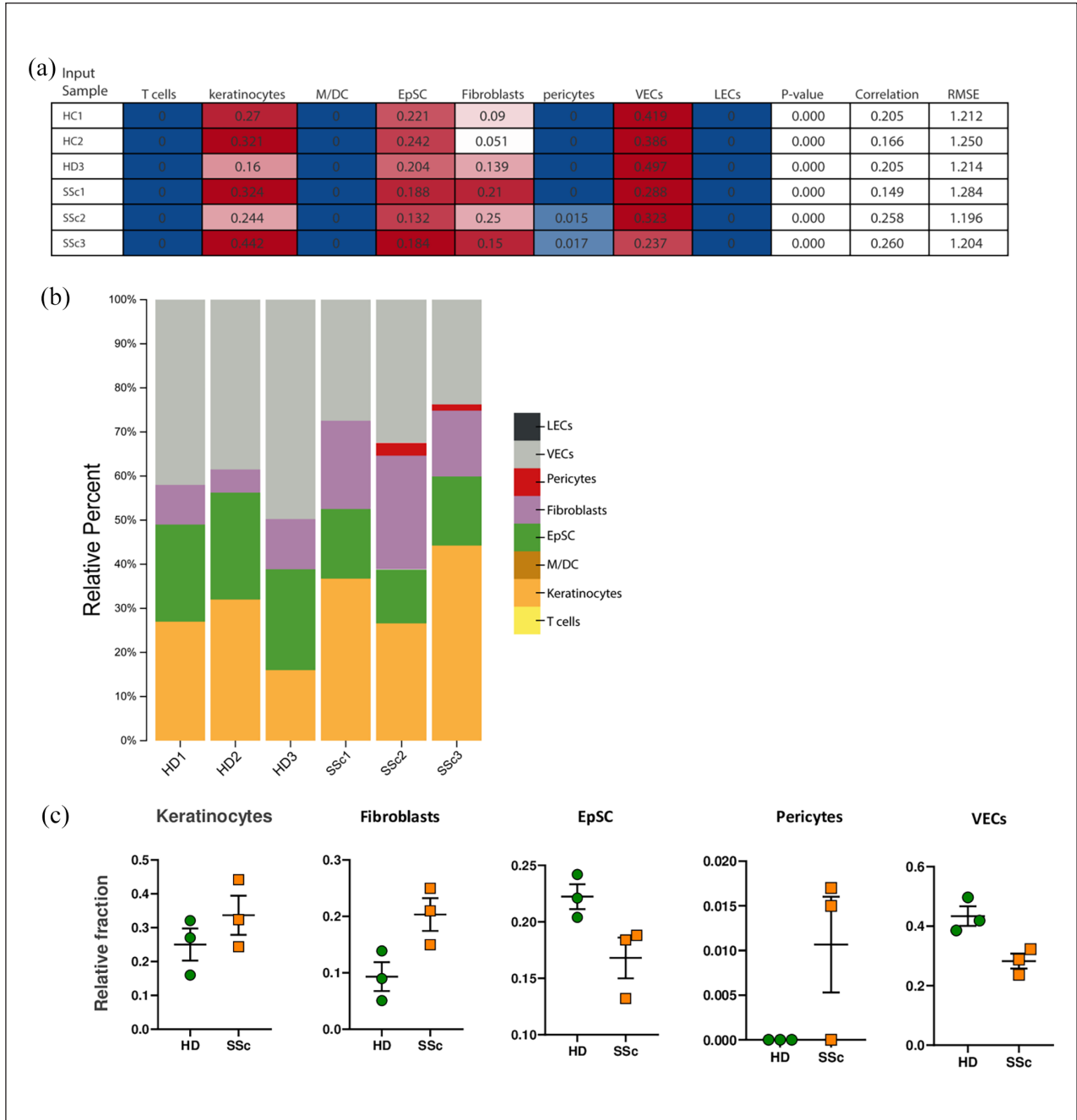


Figure 4. Cell subsets according to the CIBERSORTx algorithm: (a) cell types expressing DEGs obtained by RNA-seq. Columns represent the cell types from the signature genes file and rows represent deconvolution results for each mixture sample. All results are reported as relative fractions normalized to 1 across all cell subsets. M/DC, macrophages/dendritic cells; EpSC, epithelial stem cells; VECs, vascular endothelial cells; LECs, lymphatic endothelial cells; *p* value, statistical significance of the deconvolution result across all cell subsets; correlation, Pearson’s correlation coefficient (*R*), generated from comparing the original mixture with the estimated mixture; RMSE, root mean squared error between the original mixture and the imputed mixture. (b) Bar chart showing the relative percentage (relative fractions × 100) of each cell type computed by CIBERSORTx. (c) Dotplots show the computed relative cellular fractions reported in A.

Declaration of conflicting interests

The author(s) declared no potential conflicts of interest with respect to the research, authorship, and/or publication of this article.

Funding

The author(s) received no financial support for the research, authorship, and/or publication of this article.

ORCID iDs

Marco de Pinto  <https://orcid.org/0000-0002-0947-8663>

Melba Lattanzi  <https://orcid.org/0000-0003-1230-7539>

Dilia Giuggioli  <https://orcid.org/0000-0002-0041-3695>

References

- Hachulla E and Launay D. Diagnosis and classification of systemic sclerosis. *Clin Rev Allergy Immunol* 2011; 40: 78–83.
- Van den Hoogen F, Khanna D, Fransen J, et al. 2013 Classification criteria for systemic sclerosis: an American College of Rheumatology/European league against rheumatism collaborative initiative. *Arthritis Rheum* 2013; 65: 2737–2747.
- Ferri C, Sebastiani M, Lo Monaco A, et al. Systemic sclerosis evolution of disease pathomorphosis and survival. Our experience on Italian patients' population and review of the literature. *Autoimmun Rev* 2014; 13(10): 1026–1034.
- Cutolo M, Soldano S and Smith V. Pathophysiology of systemic sclerosis: current understanding and new insights. *Expert Rev Clin Immunol* 2019; 15(7): 753–764.
- Di Benedetto P, Ruscitti P, Liakouli V, et al. The vessels contribute to fibrosis in systemic sclerosis. *Isr Med Assoc J* 2019; 21(7): 471–474.
- Matucci-Cerinic M, Kahaleh B and Wigley FM. Review: evidence that systemic sclerosis is a vascular disease. *Arthritis Rheum* 2013; 65(8): 1953–1962.
- Altork N, Wang Y and Kahaleh B. Endothelial dysfunction in systemic sclerosis. *Curr Opin Rheumatol* 2014; 26: 615–620.
- van Bon L, Affandi AJ, Broen J, et al. Proteome-wide analysis and CXCL4 as a biomarker in systemic sclerosis. *N Engl J Med* 2014; 370: 433–443.
- Manetti M, Guiducci S, Romano E, et al. Overexpression of VEGF165b, an inhibitory splice variant of vascular endothelial growth factor, leads to insufficient angiogenesis in patients with systemic sclerosis. *Circ Res* 2011; 109: e14–e26.
- Newman AM, Steen CB, Liu CL, et al. Determining cell type abundance and expression from bulk tissues with digital cytometry. *Nat Biotechnol* 2019; 37(7): 773–782.
- Apostolidis SA, Stifano G, Tabib T, et al. Single cell RNA sequencing identifies HSPG2 and APLNR as markers of endothelial cell injury in systemic sclerosis skin. *Front Immunol* 2018; 9: 2191.
- Deng CC, Hu YF, Zhu DH, et al. Single-cell RNA-seq reveals fibroblast heterogeneity and increased mesenchymal fibroblasts in human fibrotic skin diseases. *Nat Commun* 2021; 12(1): 3709.
- Liu X, Chen W, Zeng Q, et al. Single-cell RNA-sequencing reveals lineage-specific regulatory changes of fibroblasts and vascular endothelial cells in keloids. *J Invest Dermatol* 2022; 142(1): 124–135.
- Soret P, Le Dantec C, Desvaux E, et al. A new molecular classification to drive precision treatment strategies in primary Sjögren's syndrome. *Nat Commun* 2021; 12(1): 3523.
- Gaydosik AM, Tabib T, Domsic R, et al. Single-cell transcriptome analysis identifies skin-specific T-cell responses in systemic sclerosis. *Ann Rheum Dis* 2021; 80(11): 1453–1460.
- Eyries M, Siegfried G, Ciumas M, et al. Hypoxia-induced apelin expression regulates endothelial cell proliferation and regenerative angiogenesis. *Circ Res* 2008; 103: 432–440.
- Kang Y, Kim J, Anderson JP, et al. Apelin-APJ signaling is a critical regulator of endothelial MEF2 activation in cardiovascular development. *Circ Res* 2013; 113: 22–31.
- Baiocchini A, Montaldo C, Conigliaro A, et al. Extracellular matrix molecular remodeling in human liver fibrosis evolution. *PLoS ONE* 2016; 11(3): e0151736.
- Laplante P, Raymond MA, Gagnon G, et al. Novel fibrogenic pathways are activated in response to endothelial apoptosis: implications in the pathophysiology of systemic sclerosis. *J Immunol* 2005; 174: 5740–5749.
- Valenzi E, Bulik M, Tabib T, et al. Single-cell analysis reveals fibroblast heterogeneity and myofibroblasts in systemic sclerosis-associated interstitial lung disease. *Ann Rheum Dis* 2019; 78(10): 1379–1387.
- Adams TS, Schupp JC, Poli S, et al. Single-cell RNA-seq reveals ectopic and aberrant lung-resident cell populations in idiopathic pulmonary fibrosis. *Sci Adv* 2020; 6(28): eaba1983.
- Schupp JC, Adams TS, Cosme C, et al. Integrated single-cell atlas of endothelial cells of the human lung. *Circulation* 2021; 144(4): 286–302.
- Rodor J, Chen SH, Scanlon JP, et al. Single-cell RNA-seq profiling of mouse endothelial cells in response to pulmonary arterial hypertension. *Cardiovasc Res* 2021; 118: 2519–2534.
- Ferri C, Arcangeletti MC, Caselli E, et al. Insights into the knowledge of complex diseases: environmental infectious/toxic agents as potential etiopathogenetic factors of systemic sclerosis. *J Autoimmun* 2021; 124: 102727.
- Ferri C, Giuggioli D, Guiducci S, et al. Systemic sclerosis Progression INvestiGation (SPRING) Italian registry: demographic and clinico-serological features of the scleroderma spectrum. *Clin Exp Rheumatol* 2020; 38 (3 Suppl. 125): 40–47.
- Giuggioli D, Manfredi A, Lumetti F, et al. Scleroderma skin ulcers definition, classification and treatment strategies our experience and review of the literature. *Autoimmun Rev* 2018; 17(2): 155–164.
- Pignatti M, Spinella A, Cocchiara E, et al. Autologous fat grafting for the oral and digital complications of systemic sclerosis: results of a prospective study. *Aesthetic Plast Surg* 2020; 44(5): 1820–1832.

28. Starnoni M, Pappalardo M, Spinella A, et al. Systemic sclerosis cutaneous expression: management of skin fibrosis and digital ulcers. *Ann Med Surg* 2021; 71: 102984.
29. Occhipinti M, Bruni C, Camiciottoli G, et al. Quantitative analysis of pulmonary vasculature in systemic sclerosis at spirometry-gated chest CT. *Ann Rheum Dis* 2020; 79(9): 1210–1217.
30. Giuggioli D, Bruni C, Cacciapaglia F, et al. Pulmonary arterial hypertension: guidelines and unmet clinical needs. *Reumatismo* 2021; 72(4): 228–246.
31. Lo Tartaro D, De Biasi S, Forcato M, et al. Gene expression analysis of T-Cells by single-cell RNA-Seq. *Methods Mol Biol* 2021; 2285: 277–296.